COMPARING DIFFERENT STRUCTURES AND ALGORITHMS IN APPLICATION TO ACTIVE NOISE CONTROL IN AN ACOUSTIC DUCT[†]

Dariusz Bismor

Institute of Automatic Control, Silesian Technical University, Gliwice, Poland

D.Bismor@ia.polsl.gliwice.pl

ABSTRACT

The goal of the paper is to present results on research on applying different algorithms and structures to active noise control in an acoustic duct. A few modifications of Least Mean Squares (LMS) algorithm are presented and compared. Two different variations of feedforward control structure has been considered.

1. INTRODUCTION

One of possible approaches to active noise control is based on identification and adaptive control methods. Big advantage of this approach is that it does not require wide and accurate knowledge about acoustic plant and gives the opportunity to easily transform algorithms used on the field of automation to active noise control. The goal of this paper is to summarize works on comparing different structures and algorithms applied to active noise control. All described experiments were arranged in a laboratory station newly built in Institute of Automatic Control of Silesian Technical University.

2. LABORATORY STATION OVERVIEW

The laboratory station block diagram is shown on Fig. 1. The duct, made of wood, is 4 meters long. It is equipped with two loudspeakers and two microphones. The loudspeaker L2 is the cancellation one. The microphone M1 is used for feedforward control and microphone M2 is the error microphone.

The input signals, obtained from microphones, are amplified and then processed by DSP board with TMS320C30 device. The output signals are amplified and send to loudspeakers.

The most important acoustic paths are from loudspeaker L2 to microphone M1 and from L2 to M2. The former introduces the acoustic feedback phenomena and the latter is responsible for secondary path effects.

For all experiments described below sampling frequency of 2kHz was used.

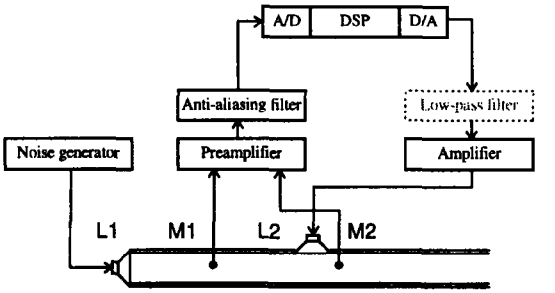

Fig. 1. Laboratory station block diagram

3. PERFORMANCE TESTS

To compare the quality of active noise control of different structures and algorithms performance tests were done. The input noise signal was generated by DPS board as a single sinusoid. The output signal from microphone M2 (Fig. 1) was measured twice: before and after switching on the control. Attenuation factor was computed as in Eq. 1:

$$\Im = 20\log\frac{\overline{o(i)}_{before}}{\overline{o(i)}_{after}} \quad [dB] \qquad (1)$$

where $o(i)$ means microphone M2 signal value in discrete-time i and dash means time averaging.

4. ALGORITHMS CONSIDERED

Before discussing algorithms presented in this paper let's have a look at the block diagram of control structure (Fig. 2). Noise signal produced by loudspeaker L1 (compare Fig. 1) is measured to obtain electrical signal $d(i)$. This signal is used by adaptive FIR filter F(i) to produce control signal $u(i)$. It is also used by adaptation mechanism together with measured error signal $e(i)$ to update adaptive filter coefficients.

[†] These research was partially supported by The Polish Committee of Scientific Research (KBN) under Grant no. 8T11A 006 11

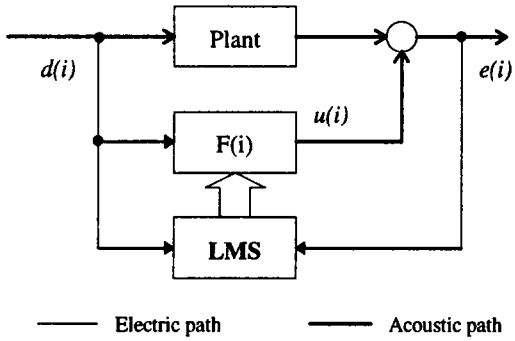

Fig. 2. Control structure block diagram.

4.1 Normalized LMS Algorithm

The basic algorithm used to active noise control is Least Mean Squares algorithm (LMS). However, choosing step size for this algorithm may lead to very long convergence times or to large steady state errors. Therefore Normalized Least Mean Squares algorithm (NLMS - Eq. 2.) was chosen as a base for this research.

$$\mathbf{F}(i+1) = \mathbf{F}(i) + \mu(i)\mathbf{d}(i)e(i),$$
$$\mu(i) = \frac{\mu}{L\hat{P}_d(i)}, \qquad (2)$$
$$\hat{P}_d(i) = (1-\alpha)\hat{P}_d(i-1) + \alpha d^2(i)$$

Normalization is done here by adjusting step size with adaptive filter length L and input signal power estimate $\hat{P}_d(i)$. The results obtained with this method are presented on Fig. 3.

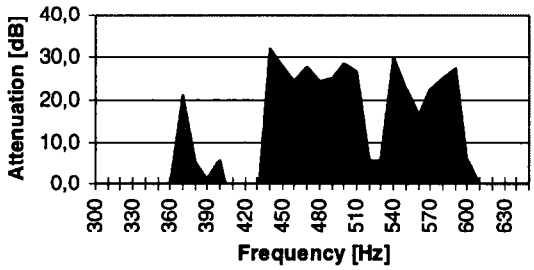

Fig. 3. Results of experiments with NLMS algorithm

4.2 Leaky LMS Algorithm

One of the best known modifications of LMS is leaky LMS algorithm (LLMS). Introducing leakage factor ν (Eq. 3) usually causes extension of attenuation band while not affecting or affecting only a bit attenuation factor. Fig. 4 shows attenuation factor for LLMS algorithm with ν equal to 0.9999.

$$\mathbf{F}(i+1) = \nu\mathbf{F}(i) + \mu(i)\mathbf{d}(i)e(i) \qquad (3)$$

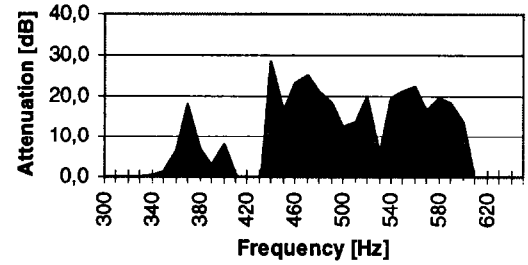

Fig. 4. Results of experiments with LLMS algorithm

4.3 Correlation LMS Algorithm

Another modification is known as correlation LMS (CLMS - Eq. 4). It allows to obtain low steady state error, because step size is based on correlation between input signal and error signal, witch is equal to zero after convergence.

$$\mathbf{F}(i+1) = \mathbf{F}(i) + \mu(i)\mathbf{d}(i)e(i)$$
$$\mu(i) = \alpha\rho(i) \qquad (4)$$
$$\rho(i) = \beta\rho(i-1) + (1-\beta)d(i)e(i)$$

The results of attenuation with CLMS algorithm are shown on Fig. 5.

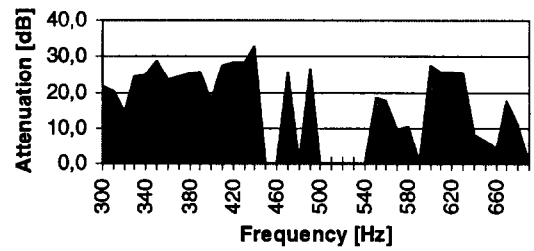

Fig. 5. Results of experiments with CLMS algorithm

4.4 Filtered-x LMS Algorithm

It is easy to notice that control structure block diagram presented on Fig. 3 is a simplification of reality. It does not contain many additional transfer functions as an electric path transfer function or transfer function between summing point and error signal measure point. This transfer functions may appear in unexpected way causing so called secondary path effects. To prevent secondary path effects, filtered-X LMS algorithm (FXLMS) is used. This algorithm is based on filtering the input signal by an estimate of the secondary path, as shown on Fig. 6. Of course, identification of secondary path must be done prior to the experiments. In this case

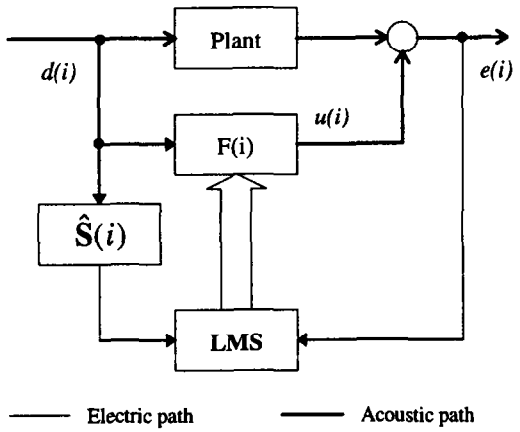

Fig. 6. Control structure block diagram for FXLMS algorithms

an ARX model of 8th degree was used as its estimate. Although any of described above modifications of LMS algorithm can be used along with structure shown on Fig. 7, only results of experiments with correlation LMS are presented on Fig. 7.

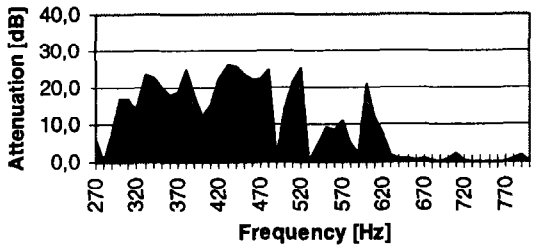

Fig. 7. Results of experiments with FXLMS algorithm

4.5 Feedback Neutralization

The main difference between classical automation applications and active noise control ones is existence of acoustical feedback between cancellating source and detector microphone (L2 and M1 on Fig. 1). This feedback may even cause unstability of the whole system. To prevent such situation acoustical feedback cancellation (neutralization) is often implemented (Fig. 8). Certainly, identification of transfer function between canceling loudspeaker and detector microphone is necessary. As in FXLMS case, ARX model of 8th degree was estimated before experiments. The results of experiments with feedback neutralization, using the normalized LMS algorithm, are presented on Fig. 9.

5. STRUCTURES CONSIDERED

Up to this moment the attenuation factor was measured with microphone M2 (Fig. 1) with sampling frequency 2kHz only. But it is easy to notice that

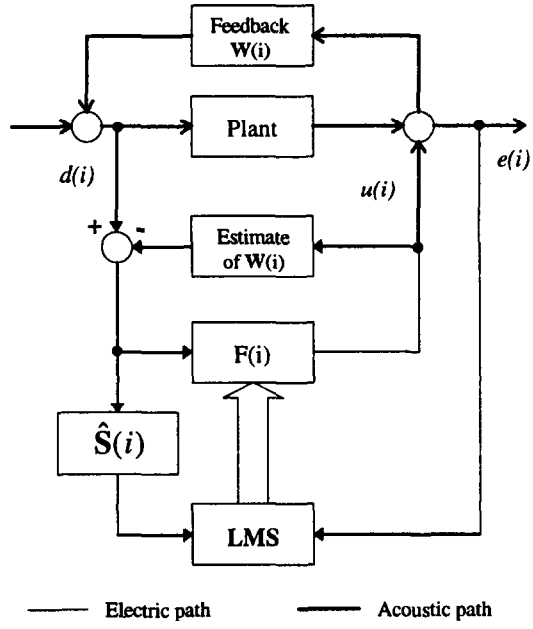

Fig. 8. Feedback neutralization block diagram

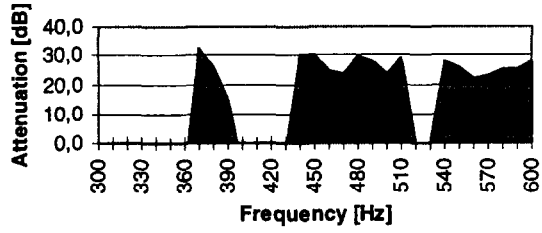

Fig. 9. Results of experiments with NLMS algorithm and feedback neutralization

generation of cancelling signal will cause existence of higher harmonics. This is because acoustic duct does not act like low-pass filter. This harmonics will not occur in measured error signal because they are over the Nyquist frequency (1kHz in this case). However, human ear is able to hear frequencies up to 20kHz! That is why the author changed the way of computing attenuation factor. In all experiments presented below Solartron-Schlumberger spectral analyzer was used to compute the energy of acoustic field in frequency range between 80Hz and 4kHz.

After changing the way of computing attenuation factor the results obtained with discussed above methods become significantly lower (see Fig. 10). Spectral analysis shown that turning on control causes the main harmonic to decrease, but also causes higher harmonics to appearing, although they were not present in noise signal. Therefore the idea was to cut the harmonics down with low-pass filter. The one used in further research was Butterworth low-pass filter with 3-dB cut-off frequency of 600Hz, and it was connected between D/A converters and power amplifier (dashed box on Fig. 1).

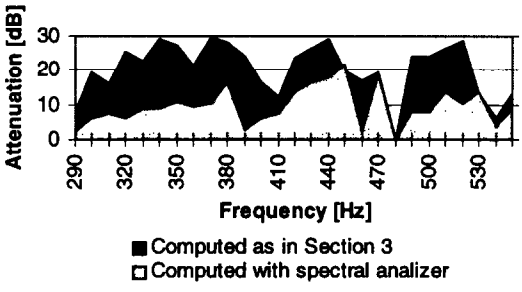

Fig. 10. Results of experiments with FXCLMS algorithm

Filtered-x correlation LMS algorithm with feedback neutralization was used for the experiments with low-pass filter. The results of tests versus the results of tests without low-pass filter are presented on Fig. 11. In this case also the difference between attenuation factor computed as in Section 3 and computed with spectral analyzer were very small.

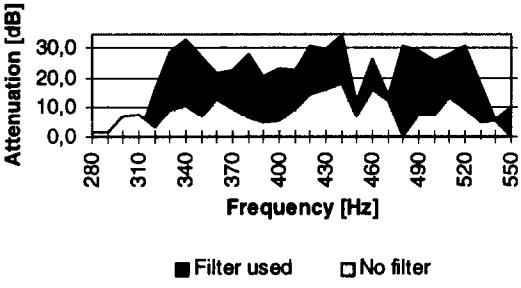

Fig. 11. Results of experiments with low-pass filter

6. REFERENCES

1. Niederlinski A.: Systemy komputerowe automatyki przemyslowej, t.2: Zastosowania, WNT, Warszawa, 1985.
2. Niederlinski A., Moscinski J., Ogonowski Z.: Regulacja adaptacyjna, PWN, Warszawa 1995.
3. Eliott S.: Active Noise and Vibration Control, Proc. Third international Symposium on Methods and Models in Automation and Robotics, Miedzyzdroje, 1996.
4. Kuo S. M., Morgan D.R.: Active noise Control Systems, John Wiley & Sons, New York, 1996.
5. Bendat, J. S., Piersol A.G.: Engineering Applications of Correlation and Spectral Analysis, John Wiley & Sons, New York, 1993.
6. Tokhi M. O.: Intelligent Active Noise and Vibration Control Methods, Proc. III Szkola Metody Aktywne Redukcji Drgan i Halasu, Kraków-Zakopane, 1997.